

Vacuum models with a linear and a quadratic term in H : structure formation and number counts analysis

Adrià Gómez-Valent, and Joan Solà

High Energy Physics Group, Dept. ECM Univ. de Barcelona,
Av. Diagonal 647, E-08028 Barcelona, Catalonia, Spain

and

Institut de Ciències del Cosmos
Univ. de Barcelona, Av. Diagonal 647, E-08028 Barcelona

E-mails: adriagova@ecm.ub.edu, sola@ecm.ub.edu

Abstract. We focus on the class of cosmological models with a time-evolving vacuum energy density of the form $\rho_\Lambda(H) = C_0 + C_1H + C_2H^2$, where H is the Hubble rate. Higher powers of H could be important for the early inflationary epoch, but are irrelevant afterwards. We study these models at the background level and at the perturbations level, both at the linear and at the nonlinear regime. We find that those with $C_0 = 0$ are seriously hampered, as they are unable to fit simultaneously the current observational data on Hubble expansion and the linear growth rate of clustering. This is in contrast to the $C_0 \neq 0$ models, including the concordance Λ CDM model. We also compute the redshift distribution of clusters predicted by all these models, in which the analysis of the nonlinear perturbations becomes crucial. The outcome is that the models with $C_0 = 0$ predict a number of counts with respect to the concordance model which is much larger, or much smaller, than the Λ CDM and the dynamical models with $C_0 \neq 0$. The particular case $\rho_\Lambda(H) \propto H$ (the pure lineal model), which in the past was repeatedly motivated by several authors from QCD arguments applied to cosmology, is also addressed and we assess in detail its phenomenological status. We conclude that the most favored models are those with $C_0 \neq 0$, and we show how to discriminate them from the Λ CDM.

1 Introduction

The accurate measurement of the luminosity-redshift curve of distant type Ia supernovae carried out at late 1990s by The Supernova Cosmology Project (Perlmutter et al. 1998) and The High-z Supernova Search Team (Riess et al. 1998) showed that our universe is speeding up. This positive acceleration could be produced by the presence of a tiny cosmological constant (CC) in Einstein's field equations, $\Lambda > 0$. This framework, the so-called concordance or Λ CDM model, seems to describe quite well the available cosmological data (Ade et al. 2013). Despite this, the CC, which is usually associated to the energy density carried by the vacuum, through the parameter $\rho_\Lambda = \Lambda/(8\pi G)$ (in which G is the Newtonian constant), has also been the origin of two of the most important current open problems in physics, namely the old CC problem (Weinberg 1989) and the Cosmic Coincidence problem (see e.g. the reviews by Padmanabhan 2003, Peebles & Ratra 2003, Copeland, Sami & Tsujikawa 2006). The severity of these problems are the main motivation to search for alternative frameworks capable to offer a more satisfactory explanation for them while still keeping a good fit to the observational data.

Different scenarios have been proposed in order to alleviate this situation, to wit: scalar fields, e.g. quintessence, modified gravity theories, decaying vacuum models, etc (cf. the previous review articles and references therein). The present work takes the point of view that the vacuum energy density is a dynamical variable in QFT in curved spacetime as in such framework it should be possible to better tackle the basic CC problems¹. Our aim here is mainly phenomenological and hence of eminently practical nature. We extend the analysis performed in (Basilakos, Plionis & Solà 2009; Grande, Solà, Basilakos & Plionis 2011; Gómez-Valent, Solà & Basilakos 2014), where some dynamical vacuum models based on powers of the Hubble rate were studied at the background and perturbation level – see also (Solà & Stefancic 2005, 2006).

In this article we focus on the dynamical vacuum models that include a linear and a quadratic term in H , i.e. $\rho_\Lambda(H) = C_0 + C_1H + C_2H^2$. We discuss the various possibilities, in particular we examine the phenomenological status of the models where no additive term C_0 is present. Of especial significance is to check out the purely linear model $\rho_\Lambda \propto H$, which is a particular case of the $C_0 = 0$ models. The linear model was amply discussed several times in the literature by different authors from different points of view. It was theoretically motivated as a possible fundamental description of the cosmological vacuum energy in terms of QCD – see e.g. (Schutzhold 2002; Klinkhamer & Volovik 2009; Thomas, Urban & Zhitnitsky 2009; Ohta 2011). Phenomenological analysis claiming its possible interest for the description of the current Universe were carried out e.g. in (Borges et al. 2008; Alcaniz et al. 2012; Chandrachani *et al.* 2014). We shall revisit the linear model here, but only as a particular case of the larger class of dynamical vacuum models that we analyze. We put to the test all these models in the light of the recent observational data and assess which are the most favored ones².

The layout of this paper is as follows. We address the background solution of the different

¹For a recent review of the idea of dynamical vacuum energy, see (Solà, 2013) and references therein, and also (Solà & Gómez-Valent, 2015) for additional considerations.

²A generalization of the vacuum structure of these models with higher powers of the Hubble rate, i.e. H^n ($n > 2$), has been recently used to describe inflation in the early universe, see e.g. (Lima, Basilakos & Solà 2013, 2014).

models in Section 2. The matter perturbations (linear and nonlinear) are considered in Section 3. The confrontation with the linear structure data is performed in Sect. 4, whereas in section 5 we probe the models with the number counts method, which requires the nonlinear analysis of structure formation. In Section 6, we present our conclusions. Finally, in the Appendix A we briefly extend the discussion of the linear model.

2 Different types of vacuum models with linear term in H

Let us consider a (spatially) flat FLRW universe. From Einstein's field equations, i.e. $G_{\mu\nu} = 8\pi G T_{\mu\nu}$, one can derive Friedmann's equation and the pressure equation by taking the 00 and the ij component, respectively:

$$3H^2 = 8\pi G(\rho_\Lambda + \rho_m), \quad (1)$$

$$3H^2 + 2\dot{H} = -8\pi G(p_\Lambda + p_m), \quad (2)$$

where the overdot denotes a derivative with respect to the cosmic time. If we are interested in describing the structure formation process, we can limit ourselves to consider only the contributions of cold matter, $p_m = 0$, and a true dynamical vacuum term, $p_\Lambda = -\rho_\Lambda$. Effects of radiation will be included in a subsequent stage, when they will be necessary. Combining Eqs. (1) and (2) it is easy to obtain the equation of local covariant conservation of the energy for a pressureless matter fluid:

$$\dot{\rho}_m + 3H\rho_m = -\dot{\rho}_\Lambda. \quad (3)$$

From these equations we can also obtain the evolution law for the Hubble function:

$$\dot{H} + \frac{3}{2}H^2 = 4\pi G\rho_\Lambda = \frac{\Lambda}{2}. \quad (4)$$

The universe's dynamics depends on the specific dynamical nature of ρ_Λ . In the present paper we study the following dynamical vacuum models³:

$$\begin{aligned} \text{I :} \quad \rho_\Lambda(H) &= \frac{3\epsilon H_0}{8\pi G} H \\ \text{II :} \quad \rho_\Lambda(H) &= \frac{3}{8\pi G} (\epsilon H_0 H + \nu H^2) \\ \text{III :} \quad \rho_\Lambda(H) &= \frac{3}{8\pi G} (c_0 + \epsilon H_0 H) \\ \text{IV :} \quad \rho_\Lambda(H) &= \frac{3}{8\pi G} (c_0 + \epsilon H_0 H + \nu H^2). \end{aligned} \quad (5)$$

Notice that the parameter $c_0 \equiv (8\pi G/3) C_0$ has dimension 2 (i.e. mass squared) in natural units. We have introduced the dimensionful constant H_0 (the value of the Hubble function at present) as a part of the linear term, and in this way the parameter ϵ in front of it can be dimensionless. Similarly ν is dimensionless since it is the coefficient of H^2 . Obviously models I, II and III are particular cases of IV, i.e. they can be obtained from IV just by setting $c_0 = \nu = 0$, $c_0 = 0$ and

³For recent related studies, see (Basilakos, Plionis & Solà 2009; Basilakos 2009; Grande, Solà, Basilakos & Plionis 2011; and Gómez-Valent, Solà & Basilakos 2014).

$\nu = 0$, respectively. However, it is convenient to study the different implementations separately because they are not phenomenological alike, and some of them are actually unfavored.

On inspecting the structure of these models, it is even questionable that theoretically all these possibilities are admissible. For example, the presence of a linear term $\propto H$ in the structure of $\rho_\Lambda(H)$ deserves some considerations. This term does not respect the general covariance of the effective action of QFT in curved spacetime (Shapiro & Solà, 2009). The reason is that it involves only one time derivative with respect to the scale factor. In contrast, the quadratic terms $\propto H^2$ involve two derivatives and hence it can be consistent with covariance. From this point of view one expects that the term $\propto H^2$ is a primary structure in a dynamical ρ_Λ model, whereas $\propto H$ is not. Still, we cannot exclude a priori the presence of the linear terms since they can be of phenomenological interest. For example, they could mimic bulk viscosity effects (cf. Barrow 1983; Zimdahl 1996; Ren & Meng 2006; Komatsu & Kimura 2013).

The first task to do in order to analyze the above models is to solve the background cosmological equations. In the following we provide the solution of model IV, which is the more general one. However, in this model the Hubble function and the energy densities cannot be solved explicitly in terms of the scale factor, only in terms of the cosmic time. This feature also holds for model III. Models I and II, however, can be solved analytically also as a function of the scale factor and we will do it because it is more convenient.

For all these models we have the following relation between the basic parameters c_0 , ν and ϵ , which follows from imposing that the dynamical vacuum energy density $\rho_\Lambda(H)$ must coincide with the current value ρ_Λ^0 at present t_0 (the point where $H(t_0) = H_0$):

$$c_0 = \frac{8\pi G}{3}\rho_\Lambda^0 - H_0^2(\epsilon + \nu) = H_0^2(\Omega_\Lambda^0 - \epsilon - \nu). \quad (6)$$

If we apply Eq. (4) to the general type-IV models, we find

$$\frac{2}{3}\dot{H} + \zeta H^2 - \epsilon H_0 H = c_0, \quad (7)$$

where we have defined $\zeta \equiv 1 - \nu$. Upon direct integration we obtain the Hubble function as a hyperbolic function of the cosmic time:

$$H(t) = \frac{H_0}{2\zeta} \left[\mathcal{F} \coth \left(\frac{3}{4} H_0 \mathcal{F} t \right) + \epsilon \right], \quad (8)$$

with

$$\mathcal{F}(\Omega_\Lambda^0, \epsilon, \nu) \equiv \sqrt{\epsilon^2 + 4\zeta(\Omega_\Lambda^0 - \epsilon - \nu)}. \quad (9)$$

Using (8) in the expression of $\rho_\Lambda(H)$ for type-IV models we can infer the vacuum energy density in terms of t

$$\rho_\Lambda(t) = \frac{3H_0^2}{32\pi G\zeta^2} \left[\mathcal{F}^2 + \epsilon^2 + 2\epsilon\mathcal{F} \coth \left(\frac{3}{4} H_0 \mathcal{F} t \right) + \nu\mathcal{F}^2 \operatorname{csch}^2 \left(\frac{3}{4} H_0 \mathcal{F} t \right) \right]. \quad (10)$$

Inserting equations (8) and (10) into Friedmann's equation (1) we can also derive the time evolution of the pressureless matter density:

$$\rho_m(t) = -\frac{\dot{H}(t)}{4\pi G} = \frac{3H_0^2}{32\pi G\zeta} \mathcal{F}^2 \operatorname{csch}^2 \left(\frac{3}{4} H_0 \mathcal{F} t \right). \quad (11)$$

The scale factor $a(t)$ can be obtained by integration of Eq. (8):

$$a(t) = B^{-\frac{1}{3\zeta}} e^{\frac{\epsilon H_0}{2\zeta} t} \sinh^{\frac{2}{3\zeta}} \left(\frac{3}{4} H_0 \mathcal{F} t \right), \quad (12)$$

with the normalization constant ($a(t_0) = 1$):

$$B = \left[\frac{[(2\zeta - \epsilon)^2 - \mathcal{F}^2]^{1 + \frac{\epsilon}{\mathcal{F}}}}{\mathcal{F}^2 (\mathcal{F} + 2\zeta - \epsilon)^{\frac{2\epsilon}{\mathcal{F}}}} \right]^{-1}. \quad (13)$$

From (12) one sees that, in general, it is not possible to eliminate the cosmic time in terms of the scale factor. It is only possible if $\epsilon = 0$ and/or $c_0 = 0$.

Let us remark that for models III and IV the values of ϵ and ν should necessarily be small since they parametrize a mild dynamical departure from the Λ CDM which we know it fits reasonably well the data. The dynamical vacuum function $\rho_\Lambda(H)$ in these models stays around the constant value ρ_Λ^0 for H near H_0 and hence ϵ and ν must be small in absolute value. This situation is of course possible because for these models $c_0 \neq 0$. Put another way: models III and IV have a smooth Λ CDM limit for $c_0 \rightarrow 0$, in contrast to models I and II. As we shall see in Sect. 4, the confrontation of models III and IV against observations does indeed confirm that $|\epsilon|$ and $|\nu|$ are in the ballpark of $\sim 10^{-3}$ (see Table 1). Quite in contrast, for models I and II ϵ and ν cannot be arbitrarily small since $\rho_\Lambda(H)$ for these models is not protected by the nonvanishing additive term c_0 . For them, the constraint (6) implies that the following relations must hold:

$$\text{I: } \epsilon = \Omega_\Lambda^0 \quad (\nu = 0) \quad \text{II: } \epsilon + \nu = \Omega_\Lambda^0. \quad (14)$$

It is thus clear that in model I there is no free parameter (apart from Ω_m^0 or Ω_Λ^0), and for model II we find that if ϵ is small, ν cannot be small, and vice versa.

Obviously models I and II satisfy one of the aforementioned conditions for which the solution in terms of the scale factor is possible, so let us provide such analytical solution in this case. The constraints (14) entail that the quantity \mathcal{F} defined in (9) boils down to $\mathcal{F} \rightarrow \epsilon$, and this allows to combine the exponential factor and the hyperbolic function in (12). The result for model II reads:

$$a(t) = \left(\frac{\Omega_m^0}{\zeta - \Omega_m^0} \right)^{2/3\zeta} \left[e^{3(\zeta - \Omega_m^0)H_0 t/2} - 1 \right]^{2/3\zeta}. \quad (15)$$

From here we can invert and derive $t(a)$, and then substitute in (8) to obtain the normalized Hubble rate to its current value, i.e. $E(a) \equiv H(a)/H_0$, for type-II models:

$$E(a) = 1 + \frac{\Omega_m^0}{\zeta} \left(a^{-3\zeta/2} - 1 \right). \quad (16)$$

We can also furnish analytical expressions for the matter and vacuum energy densities as a function of the scale factor:

$$\rho_m(a) = \rho_c^0 \left[\zeta E^2(a) - (\zeta - \Omega_m^0) E(a) \right] = \rho_m^0 f(a) a^{-3\zeta}, \quad (17)$$

where

$$f(a) = a^{3\zeta/2} E(a) = \frac{\Omega_m^0}{\zeta} + \left(1 - \frac{\Omega_m^0}{\zeta} \right) a^{3\zeta/2}, \quad (18)$$

and

$$\rho_\Lambda(a) = \rho_c^0 [(1 - \zeta) E^2(a) + (\zeta - \Omega_m^0) E(a)] . \quad (19)$$

Here ρ_c^0 is the current critical density, i.e. $\rho_c^0 = 3H_0^2/8\pi G$. The corresponding expressions for type-I model can be directly extracted from (16), (17) and (19) by setting $\zeta = 1$):

$$H(a) = H_0 \left[1 + \Omega_m^0 (a^{-3/2} - 1) \right] , \quad (20)$$

$$\rho_m(a) = \rho_m^0 \left[\Omega_m^0 + (1 - \Omega_m^0) a^{3/2} \right] a^{-3} , \quad (21)$$

$$\rho_\Lambda(a) = \rho_\Lambda^0 \frac{H(a)}{H_0} = \rho_\Lambda^0 \left[1 + \Omega_m^0 (a^{-3/2} - 1) \right] . \quad (22)$$

The first term on the *r.h.s.* of Eq. (17) is the dominant one at high redshifts ($z \gg 1$, equivalently $a \ll 1$). Therefore, in this regime the matter density evolves like $\rho_m \propto \Omega_m^{(0)2} a^{-3\zeta} \propto \Omega_m^{(0)2} (1+z)^{3\zeta}$. A similar scaling law is found for type-I models, with $\zeta = 1$.

The following observation is in order. In the concordance model we have the standard behavior of the matter density $\rho_m(z) = \rho_m^0 (1+z)^3$, but when we compare it with (17) and (21) we observe that for type-I and II models there is an extra factor of Ω_m^0 . This factor stands out maximally in the remote past where for the same value of ρ_m the type-I and type-II models should predict a larger matter density Ω_m^0 at present (cf. Appendix A). The reason is obvious: if a term of order $(\Omega_m^0)^2$ should mimic the standard value $(\Omega_m^0)^{\Lambda\text{CDM}} \simeq 0.3$, the value itself of Ω_m^0 must be of order ~ 0.5 and hence significantly larger ($\sim 70\%$) than the standard one. This situation does not occur so acutely for the low and intermediate redshift range, as can be seen e.g. from Eq. (21) for model I, where for $a \simeq 1$ the two terms in the square brackets add up approximately to 1 and we recover the ΛCDM behavior $\rho_m \sim \rho_m^0 a^{-3}$. As we will comment in Sect. 4, we find more appropriate to test these ‘‘anomalous’’ models near the region where they can mimic the ΛCDM to some reasonable extent, i.e. at relatively low redshifts.

Up to now, we have not included the effect of relativistic matter since we were interested in studying the background solutions near our time and the physics of cosmological perturbations. In spite of this, when we will put our models to the test the radiation correction must be taken into account in our overall fit to the main cosmological data, especially in regard to the data on Baryonic Acoustic Oscillations (BAOs) and Cosmic Microwave Background (CMB). In fact, when the CMB was released ($z_* \sim 1100$) the amount of radiation was not negligible, so we had better include the relativistic matter component in our analysis. The generalized energy conservation law involving also radiation reads as follows:

$$\dot{\rho}_m + \dot{\rho}_r + 3H\rho_m + 4H\rho_r = -\dot{\rho}_\Lambda . \quad (23)$$

We may compute $\dot{\rho}_\Lambda$ in this expression from the explicit form of the general vacuum energy in Eq. (5), i.e. using model IV. Since relativistic and non-relativistic matter are in interaction one can split the obtained expression with the aid of an interaction source $Q(t)$:

$$\begin{aligned} \dot{\rho}_m + 3\rho_m \left[\zeta H - \frac{\epsilon}{2} H_0 \right] &= Q(t) , \\ \dot{\rho}_r + 4\rho_r \left[\zeta H - \frac{\epsilon}{2} H_0 \right] &= -Q(t) . \end{aligned} \quad (24)$$

Notice that when one of the matter components dominates over the other we are allowed to turn the source $Q(t)$ off and solve the decoupled system. The corresponding results for non-relativistic and relativistic matter are as follows:

$$\rho_m(t, a) = \rho_m^0 e^{\frac{3}{2}\epsilon H_0(t-t_0)} a^{-3\zeta}, \quad (25)$$

$$\rho_r(t, a) = \rho_r^0 e^{2\epsilon H_0(t-t_0)} a^{-4\zeta}. \quad (26)$$

The presence of the time dependence in the exponential, which is triggered by the ϵ -parameter of the linear term in the vacuum function, is reminiscent of the fact that for models III and IV the energy densities cannot be expressed fully in terms of the scale factor.

In good approximation we can assume that the evolution of the scale factor as of the time when the CMB was released corresponds to the cold matter epoch, i.e. we suppose it is evolving as indicated in Eq. (12). In this way we can determine the energy densities (25) and (26) in terms of the cosmic time only. This last step can be performed analytically only if we suppose that the effects of radiation are sufficiently small, as it is indeed the case under consideration. We find:

$$\rho_m(t) = \rho_m^0 B e^{-\frac{3}{2}\epsilon H_0 t_0} \operatorname{csch}^2 \left(\frac{3}{4} H_0 \mathcal{F} t \right), \quad (27)$$

$$\rho_r(t) = \rho_r^0 B^{4/3} e^{-2\epsilon H_0 t_0} \operatorname{csch}^{8/3} \left(\frac{3}{4} H_0 \mathcal{F} t \right), \quad (28)$$

where the constant B is the same as that in (13).

The following normalization condition must be fulfilled so that the energy densities take the present value at $t = t_0$:

$$B e^{-\frac{3}{2}\epsilon H_0 t_0} \operatorname{csch}^2 \left(\frac{3}{4} H_0 \mathcal{F} t_0 \right) = 1. \quad (29)$$

Note that we can actually determine t_0 in terms of the remaining parameters by matching equations (27) and (11):

$$B e^{-\frac{3}{2}\epsilon H_0 t_0} = \frac{\mathcal{F}^2}{4\zeta \Omega_m^0} = \frac{\epsilon^2 + 4\zeta(\Omega_\Lambda^0 - \epsilon - \nu)}{4\zeta \Omega_m^0}. \quad (30)$$

The Hubble function of the matter-dominated epoch including the radiation contribution can be calculated from the generalized Friedmann's equation for model IV:

$$H^2(t) = \frac{8\pi G}{3} [\rho_m(t) + \rho_r(t)] + c_0 + \epsilon H_0 H(t) + \nu H^2(t). \quad (31)$$

It can be checked that thanks to the condition (29) the implicit formula (31) for the Hubble function leads to the extended cosmic sum rule $\Omega_m^0 + \Omega_r^0 + \Omega_\Lambda^0 = 1$, as expected. After some rearrangement and making use of (27) and (28), we can bring Eq. (31) into the form

$$\zeta H^2 - \epsilon H_0 H - H_0^2 s(t) = 0, \quad (32)$$

where

$$s(t) = \zeta - \epsilon - \Omega_m^0 - \Omega_r^0 + \frac{\mathcal{F}^2}{4\zeta} \operatorname{csch}^2 \left(\frac{3}{4} H_0 \mathcal{F} t \right) + \Omega_r^0 \left(\frac{\mathcal{F}^2}{4\zeta \Omega_m^0} \right)^{4/3} \operatorname{csch}^{8/3} \left(\frac{3}{4} H_0 \mathcal{F} t \right). \quad (33)$$

Model	Ω_m^0	$\nu = 1 - \zeta$	ϵ	χ^2/dof
Λ CDM	0.293 ± 0.013	-	-	567.8/586
I	$0.302^{+0.010}_{-0.009}$	-	$1 - \Omega_m^0$	575.7/585
II	$0.295^{+0.016}_{-0.011}$	$1 - \Omega_m^0 - \epsilon$	$0.93^{+0.01}_{-0.02}$	567.7/584
III	$0.297^{+0.015}_{-0.014}$	-	$-0.014^{+0.016}_{-0.013}$	587.2/585
IVa	$0.300^{+0.017}_{-0.003}$	-0.004 ± 0.002	-0.004 ± 0.002	583.1/585
IVb	$0.297^{+0.005}_{-0.015}$	-0.002 ± 0.002	-0.001 ± 0.001	579.5/585

Table 1: The fit values for the various models, together with their statistical significance according to a χ^2 -test. We have performed a joint statistical analysis of the SNIa+CMB+BAO_{dz} data for the Λ CDM, type-III and type-IV models. For type-I and type-II models, instead, we have used SNIa+BAO_A data for the reasons explained in the text. To break parameter degeneracies we present the fitting results for two different cases: the one indicated as IVa (resp. IVb) corresponds to $\nu = \epsilon$ (resp. $\nu = 2\epsilon$). Recall that because of the constraints (14) model I has Ω_m^0 as the sole free parameter, whereas for model II one can adopt Ω_m^0 and ϵ .

Thus, the sought-for Hubble function in the presence of a relatively small amount of relativistic matter can be computed by solving Eq. (32):

$$H(t) = \frac{H_0}{2\zeta} \left[\epsilon + \sqrt{\epsilon^2 + 4\zeta s(t)} \right]$$

$$H(t) = \frac{H_0}{2\zeta} \left[\epsilon + \mathcal{F} \coth \left(\frac{3}{4} H_0 \mathcal{F} t \right) \sqrt{1 + \Delta(t)} \right], \quad (34)$$

where $\Delta(t)$ is defined as

$$\Delta(t) = \frac{\Omega_r^0}{\Omega_m^0} \left(\frac{\mathcal{F}^2}{4\zeta\Omega_m^0} \right)^{1/3} \operatorname{csch}^{2/3} \left(\frac{3}{4} H_0 \mathcal{F} t \right) \operatorname{sch}^2 \left(\frac{3}{4} H_0 \mathcal{F} t \right). \quad (35)$$

In Eq. (34) we have made use of the extended cosmic sum rule mentioned above to establish the relation

$$\zeta - \epsilon - \Omega_m^0 - \Omega_r^0 = \Omega_\Lambda^0 - \nu - \epsilon = \frac{\mathcal{F}^2 - \epsilon^2}{4\zeta}. \quad (36)$$

The numerical integration of (34) provides the improved form of the scale factor for a general type-IV model, namely $a(t) = e^{\int_{t_0}^t H(\hat{t}) d\hat{t}}$. Thus, we can obtain the points of the curves $H(a)$, $\rho_m(a)$, $\rho_r(a)$ and $\rho_\Lambda(a)$ computationally using the results presented before. With this strategy we can better confront the model with observations since the data inputs are given in terms of the cosmological redshift variable $z = (1 - a)/a$.

On comparing equations (8) with (34) we immediately recognize that $\Delta(t)$ represents the correction term introduced by the effect of the radiation upon the original expression (8). Obviously $\Delta(t) \approx 0$ at the present time. However, this is not so at the decoupling time. Indeed, taking⁴ $\Omega_r^0/\Omega_m^0 = (1 + 0.227 N_\nu) \Omega_\gamma^0/\Omega_m^0 = 4.15 \times 10^{-5} (\Omega_m^0 h^2)^{-1} \simeq 3 \times 10^{-4}$, we find that $\Delta(t)$ rockets into a numerical value of order $\sim 10^3$ at the time of last scattering. The net outcome is that the fraction of relativistic matter at decoupling can be around 23 %.

⁴We include photons and $N_\nu = 3$ neutrino species, with $\Omega_m^0 h^2 \simeq 0.14$ from Planck+WP (Ade et al. 2013).

As we have seen, for type-II model (and in particular for type-I) one can derive the energy densities (25) and (26) in terms of the scale factor. The answer for nonrelativistic matter is given in Eq. (17). For radiation we can proceed in a similar way, and the result is:

$$\rho_r(a) = \rho_r^0 f^{4/3}(a) a^{-4\zeta}, \quad (37)$$

where $f(a)$ was defined in (18). The modified Hubble rate for type-II models can be expressed in terms of the scale factor by solving (31) after setting $c_0 = 0$ and using (17) and (37):

$$E(a) = \frac{\zeta - \Omega_m^0 + \sqrt{(\zeta - \Omega_m^0)^2 + 4\zeta \left[\frac{\rho_m(a) + \rho_r(a)}{\rho_e^0} \right]}}{2\zeta}. \quad (38)$$

Substituting this expression in (5)/ type II we find the corresponding vacuum energy density $\rho_\Lambda(a)$ including the effect of radiation, which is a cumbersome expression.

We can also estimate the equality time, t_{eq} , between the radiation and the non-relativistic matter energy densities for models of type I and II. Equating (17) and (37) and taking into account that $a_{eq} \ll 1$ we obtain:

$$a_{eq} = \left[\frac{\Omega_r^0}{\zeta^{1/3} (\Omega_m^0)^{2/3}} \right]^{1/\zeta}. \quad (39)$$

For the typical values that ζ and Ω_m^0 take in Table 1, a_{eq} deviates significantly from the Λ CDM prediction value $a_{eq} = \Omega_r^0/\Omega_m^0$. In contrast, for models of type-III and IV (which have $c_0 \neq 0$) one can use the concordance value as a very good approximation. In these cases one can show that $a_{eq} = \Omega_r^0/\Omega_m^0 [1 + x \ln(\Omega_r^0/\Omega_m^0) + \mathcal{O}(x^2)]$, where $x(\epsilon, \nu) \ll 1$ and the deviations from the Λ CDM model value are only at the few percent level. Needless to say, additional important differences of the $c_0 = 0$ models are expected to appear in connection to the photon decoupling and baryon drag epochs, and in the value of the comoving Hubble scale, k_{eq}^{-1} , at the redshift of matter-radiation equality (cf. sections 4 and 5 for additional considerations on these matters).

As to the behavior of the energy densities deep in the radiation epoch for type-I and II models, let us note that it can be relevant for the primordial big bang nucleosynthesis (BBN). The ratio between the vacuum and radiation energy densities for $a \ll 1$ can be estimated from the foregoing analysis, with the result:

$$\frac{\rho_\Lambda}{\rho_r} \approx \left(\frac{1 - \zeta}{\zeta} \right) \left[1 + \left(\frac{a}{a_{eq}} \right)^\zeta \right], \quad (40)$$

where use has been made of (39). Notice that the term enclosed in the square brackets provides the correction to the result that can be inferred from (17) and (19) in the matter dominated epoch at high redshift, but without radiation. Taking into account the fitted values of the parameters presented in Table 1, we find $\zeta = \epsilon + \Omega_m^0 = 1.225$. Therefore, at $a = a_{eq}$ the ratio (40) yields $\rho_\Lambda \approx -0.37\rho_m$, and at the BBN epoch (where $a \ll a_{eq}$) we have $\rho_\Lambda \approx -0.18\rho_m$. We learn from these estimates that type-II models predict a negative value of ρ_Λ in the past and, moreover, it is a non-negligible fraction of ρ_r at the BBN time. This fraction could of course be made smaller by decreasing ν (i.e. approaching $\zeta \rightarrow 1$) but this would worsen the quality of the fit since model II

provides a better fit to low energy data than model I (cf. Table I). In compensation for its poorer description of the current data, model I satisfies $\rho_\Lambda/\rho_r \rightarrow 0$ when $a \rightarrow 0$, similar to the Λ CDM, and therefore its vacuum energy is, in principle, harmless for the BBN.

3 Linear and nonlinear structure formation

For type-IV models the nonlinear equation for the growth factor $\delta_m(t) = \delta\rho_m(t)/\rho_m(t)$ can be derived after some lengthy calculations leading to the following final result⁵:

$$\begin{aligned} & \frac{9}{16}H_0^2\mathcal{F}^2(1-y)^2\delta_m'' + \frac{3}{4}H_0\mathcal{F}\delta_m'(1-y^2) \left[2H + \Psi - \frac{3}{2}yH_0\mathcal{F} \right] \\ & + \left[2H\Psi + \frac{3}{4}H_0\mathcal{F}(1-y^2)\Psi' - \frac{\rho_m}{2}(1+\delta_m) \right] \delta_m - \frac{\Psi^2\delta_m^2}{3(1+\delta_m)} \\ & - \left[\frac{4\left(\frac{3}{4}H_0\mathcal{F}(1-y^2)\delta_m'\right)^2 + \frac{15}{4}\Psi H_0\mathcal{F}(1-y^2)\delta_m\delta_m'}{3(1+\delta_m)} \right] = 0, \end{aligned} \quad (41)$$

where the variable y is related to the cosmic time through $y(t) \equiv \coth\left(\frac{3}{4}H_0\mathcal{F}t\right)$, and $\Psi \equiv -\dot{\rho}_\Lambda/\rho_m$. The primes indicate derivatives with respect to y . The expressions for $\Psi(y)$, $\rho_m(y)$ and $H(y)$ for type-IV models are, respectively:

$$\Psi(y) = -\frac{\dot{\rho}_\Lambda(t)}{\rho_m(t)} = \frac{3H_0}{2\zeta} [y(1-\zeta)\mathcal{F} + \epsilon], \quad (42)$$

$$\rho_m(y) = \frac{3H_0^2}{32\pi G\zeta}\mathcal{F}^2(y^2-1), \quad (43)$$

and

$$H(y) = \frac{H_0}{2\zeta}[\mathcal{F}y + \epsilon]. \quad (44)$$

The numerical solution of the above nonlinear equation is used to compute the collapse density threshold $\delta_c(z)$, an important model-dependent quantity that is used in the number counts analysis of Sect.5. Once more we refer the reader to (Grande, Solà, Basilakos & Plionis 2011) for details (see also Pace, Waizmann & Bartelmann 2010).

If we are, however, interested only in the linear growth factor we can throw away the nonlinear terms from (41), i.e. the $\mathcal{O}(\delta_m^2)$ terms. Let us dispense with these terms at this point, as we wish to focus on the large scale linear perturbations. In practice, to solve the resulting linear differential equation we have to fix the initial conditions for δ_m and δ_m' . We take them at very high redshift $z \gg 1$. The scale factor (12) can be expressed in terms of y :

$$a(y) = B^{-\frac{1}{3\zeta}}(y^2-1)^{-\frac{1}{3\zeta}} \left(\frac{y+1}{y-1} \right)^{\frac{\epsilon}{3\zeta\mathcal{F}}}. \quad (45)$$

For the general model IV (with $c_0 \neq 0$) we normalize the growth factor with the value $\delta_m(z=0)$, i.e. $\delta_m(a=1)$, and we take $\delta_m(a) = a$ at very high redshifts. The initial conditions at $y_i = 700$,

⁵We follow the procedure explained in detail in Appendix A of (Grande, Solà, Basilakos & Plionis 2011).

corresponding to $z_i \simeq 100$ for type-IV models, are the following. For the growth factor we have $\delta_m(y_i) = a(y_i)$, and for its derivative with respect to the y -variable, we obtain

$$\delta'_m(y_i) = \left. \frac{da(y)}{dy} \right|_{y_i} = \frac{-2a(y_i)}{3\zeta(y_i^2 - 1)} \left(y_i + \frac{\epsilon}{\mathcal{F}} \right). \quad (46)$$

Unfortunately, the differential equation for δ_m cannot be solved analytically neither for type-III nor for type-IV models. We are forced to use numerical techniques, for instance the method of finite differences, which is anyway necessary for tackling the original nonlinear equation (41). For type-II models the perturbation equations can be readily obtained by setting $c_0 \rightarrow 0$. In this limit, the y -variable reads $y = -1 + 2\zeta E/\epsilon$. Introducing now $y_1 = (y + 1)/(y - 1)$, the differential equation for the linear perturbations becomes

$$3\zeta^2 y_1 (y_1 - 1)^2 \frac{d^2 \delta_m}{dy_1^2} + 2\zeta (y_1 - 1) (5y_1 - 3\zeta) \frac{d\delta_m}{dy_1} - 2(2 - \zeta) (3\zeta - 2y_1) \delta_m = 0. \quad (47)$$

This result is consistent with that of (Basilakos & Solà 2014). A power-like solution of Eq. (47) immediately ensues: $\delta_{m-}(y_1) \sim (y_1 - 1)^{(\zeta - 2)/\zeta}$. While an explicit relation of the variable y with the scale factor is impossible for models III and IV, for type-II models the variable y_1 defined above permits such relation:

$$y_1 = \frac{\zeta E}{\zeta E - \epsilon} = 1 + \frac{\zeta - \Omega_m^0}{\Omega_m^0} a^{3\zeta/2}. \quad (48)$$

Thanks to this feature the previously found solution can be rewritten as $\delta_{m-}(a) \sim a^{3(\zeta - 2)/2}$. The latter is the decaying mode solution (since $\zeta < 2$) and, therefore, must be rejected. From it we can generate the growing mode solution for the type-II model:

$$\delta_{m+}(a) = C_1 a^{3(\zeta - 2)/2} \int_0^a \frac{da'}{a'^{3\zeta/2} E^2(a')}, \quad (49)$$

with C_1 a constant. The behavior of Eq. (49) in the early epoch, namely when $E(a) \sim (\Omega_m^0/\zeta)a^{-3\zeta/2}$, is $\delta_m(a) \sim a^{3\zeta - 2}$. In the case of model I, for which $\zeta = 1$, we have $\delta_m(a) \sim a$. This is the same limiting behavior as that of the Λ CDM model, with the proviso that that for both models with $c_0 = 0$ there is an extra factor of Ω_m^0 in the matter density. Such anomaly is not innocuous; it has dramatic consequences that will be analyzed in the next sections.

Before closing this section we should like to point out that the pure quadratic model $\rho_\Lambda \propto H^2$ (corresponding to $c_0 = \epsilon = 0$) is excluded since such model does not have an inflection point from deceleration to acceleration (cf. Basilakos, Polarski & Solà 2012). In addition, it has no growing modes for structure formation. This last part can be immediately inferred from Eq. (49) using the fact that $E(a) = a^{-3\zeta/2}$ for that model. As a result, one can easily check that the growing mode exists only for $\zeta > 2/3$ (equivalently, for $\nu < 1/3$) and in this case the Universe is always decelerating. Thus we shall not consider this model any longer in our analysis. While the pure H^2 model is excluded, we should emphasize that when it is complemented with the $c_0 \neq 0$ term, i.e. when we consider $\epsilon = 0$ in type-IV models, the resulting expression takes on the general form $\rho_\Lambda(H) = C_0 + C_2 H^2$. This structure for the vacuum energy density is perfectly viable from the phenomenological point of view, and in fact it is one of the simplest and more

attractive formulations of the dynamical vacuum compatible with the general form of the effective action in QFT since now both terms (the constant terms and the H^2 term) are allowed by general covariance⁶. The phenomenological status of this model (and some generalizations) has been confronted against data e.g. in (Basilakos, Plionis & Solà 2009; Grande, Solà, Basilakos & Plionis 2011; Basilakos, Polarski & Solà 2012) and even more recently in (Gómez-Valent, Solà & Basilakos 2014). It was discussed also in older works both theoretically and phenomenologically using the first supernovae data (España-Bonet et al. 2003; Shapiro & Solà 2002, 2003 and 2004).

4 Vacuum models and linear growth

In Table 1 we show the best-fit values for the models we are considering. For type-III and type-IV models we have used a joint statistical analysis involving the latest data, i.e. SNIa-Union2.1 (Suzuki et al. 2011), BAO measurements in terms of the parameter $d_z(z_i) = r_s(z_d)/D_V(z_i)$ (Blake et al. 2011) and the CMB shift parameter (Ade et al. 2013; Shaefer and Huterer, 2013)⁷. We have proceeded in a different manner with type-I and type-II models due to the fact that the usual fitting formulas for computing the redshifts at decoupling and the baryon drag epochs provided by (Hu & Sugiyama 1995) are tailor-made for the Λ CDM model and in general for Λ CDM-like models. While this is the case for type III and IV models, this is not so for type I and II for which the additive term is $c_0 = 0$. We have already seen in Sect. 2 that these last two types of models present some surprises in the structure of the matter density, most conspicuously the fact that at large redshift they behave $\rho_m \propto (\Omega_m^0)^2$ rather than the standard behavior $\rho_m \propto \Omega_m^0$.

For this reason, for the non Λ CDM-like models I and II we have implemented the fitting procedure by just concentrating on the low and intermediate redshifts, that is to say, we have used the type Ia supernovae data but avoided using CMB data. At the same time for these models we have used Eisenstein's BAO parameter $A(z)$ (Eisenstein, 2005), tabulated as in (Blake et al. 2011). It is given as follows:

$$A(z_i, \mathbf{p}) = \frac{\sqrt{\Omega_m^0}}{E^{1/3}(z_i)} \left[\frac{1}{z_i} \int_0^{z_i} \frac{dz}{E(z)} \right]^{2/3}. \quad (50)$$

For models I and II we have avoided to use the BAO d_z -parameter, which requires the computation of the comoving distance that light can travel up to the baryon drag epoch (at redshift z_d), i.e. the quantity

$$r_s(z_d) = \int_0^{t(z_d)} \frac{c_s dt}{a} = \int_{z_d}^{\infty} \frac{c_s(z) dz}{H(z)}, \quad (51)$$

where

$$c_s(z) = c \left(\frac{\delta p_\gamma}{\delta \rho_\gamma + \delta \rho_b} \right)^{1/2} = \frac{c}{\sqrt{3(1 + \mathcal{R}(a))}} \quad (52)$$

is the sound speed in the baryon-photon plasma. Note that this quantity is model-dependent because $\mathcal{R}(z) = \delta \rho_b / \delta \rho_\gamma$ is so. However, for models III and IV (the ones which are Λ CDM-like)

⁶For a theoretical discussion in the context of QFT in curved spacetime, see e.g. (Solà 2008; Shapiro & Solà 2009; Solà 2013).

⁷The procedure we have followed is standard, see e.g. (Basilakos, Plionis & Solà 2009; Grande, Solà, Basilakos & Plionis 2011; Gómez-Valent, Solà & Basilakos 2014) for details.

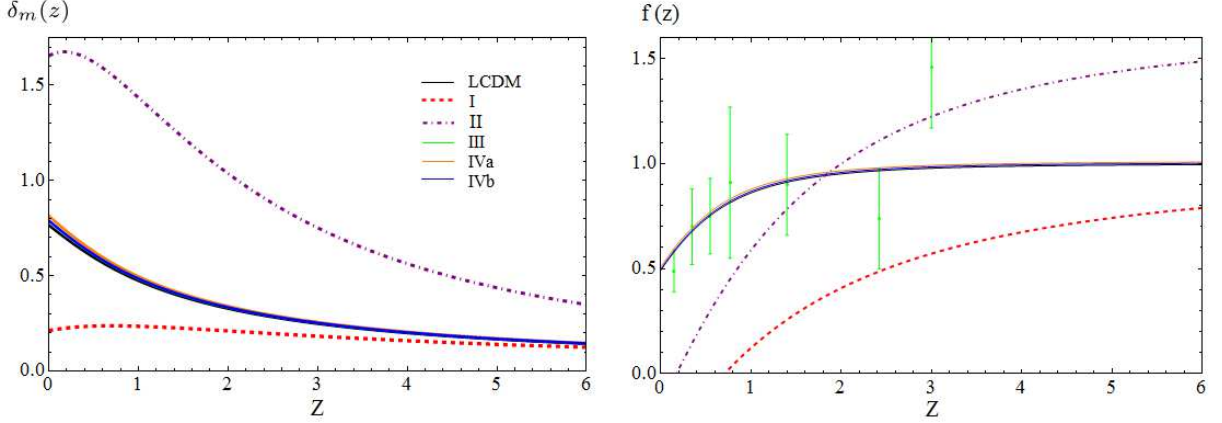


Figure 1: *Left plot:* The non-normalized density contrast $\delta_m(z)$ predicted by the various models under study, Eq. (5), using the fit values collected in Table 1; *Right plot:* Comparison of the observational data (see text) – with error bars depicted in green – and the theoretical evolution of the linear growth rate of clustering $f(z)$, confer Eq. (55), for each vacuum model. Models III and IV are almost indistinguishable from the Λ CDM one.

we can safely use the BAO d_z -parameter, also tabulated in (Blake et al. 2011), and in fact we have adopted it in such cases. The necessary corrections for these models amount to the following expression, which is obtained after using equations (27) and (28):

$$\mathcal{R}(t) = \frac{3\Omega_b^0}{4\Omega_\gamma^0} \left[\frac{\sinh\left(\frac{3}{4}H_0\mathcal{F}t\right)}{\sinh\left(\frac{3}{4}H_0\mathcal{F}t_0\right)} \right]^{2/3}. \quad (53)$$

One can easily check that for $\nu = \epsilon = 0$ we retrieve the corresponding Λ CDM result:

$$\mathcal{R}(t)|_{\epsilon=\nu=0} = \frac{3\Omega_b^0}{4\Omega_\gamma^0} a(t). \quad (54)$$

As already warned, the situation for models I and II is different as we cannot use the standard formulae for estimating z_d owing to the anomalous behavior of H at very high redshift. For this reason we have used only the BAO_A data for them (based on the aforementioned acoustic parameter $A(z)$ whose computation does not involve any integration in the very high redshift range), and of course the SNIa data. For models III and IV, in contrast, we have used SNIa and CMB data collected from the aforementioned references, and BAO_{d_z} data based on the d_z -parameter, tabulated also in (Blake et al. 2011).

Proceeding in this way we can see from Table 1 that the fitting values of Ω_m^0 associated to models I and II are not very different from those of models III and IV, and all of them are reasonably close to the Λ CDM model (which is also included in that table and fitted from the same data). From this point of view (and attending also to the χ^2 values per d.o.f.) we can say that these models perform an acceptable fit to the cosmological data. For models I and II, however, we can attest this fact only for the low and intermediate redshift data. If we include the CMB shift parameter and the BAO_{d_z} data, models I and II then peak at around $\Omega_m^0 \sim 0.5$ (and with a bad fit quality, see Appendix A). Such poor performance is caused by the aforementioned $\rho_m \propto (\Omega_m^0)^2$ anomalous behavior of these models at large redshift.

Even if we restrain to the low and intermediate redshift data for models I and II, which as we have seen lead to an acceptable value of $\Omega_m^0 \simeq 0.3$ (cf. Table 1), they nevertheless clash violently with a serious difficulty, namely they are bluntly unable to account for the linear structure formation data, as it is plain at a glance on Fig. 1 (plot on the right). The observational data in that plot have been taken from Table 1 of (Jesus et al. 2011) and references therein.

To better understand the meaning of Fig. 1, let us recall that from the standard definition of the density contrast $\delta_m = \delta\rho_m/\rho_m$ one can define the linear growth rate of clustering (Peebles 1993), as follows:

$$f(z) \equiv \frac{d \ln \delta_m}{d \ln a} = -(1+z) \frac{d \ln \delta_m(z)}{dz}. \quad (55)$$

Both $\delta_m(z)$ and $f(z)$ have been plotted in Fig. 1 for the models under study together with the Λ CDM.

The obvious departure of models I and II from the linear growth data is an important drawback for these models. It implies that the initial success in fitting the Hubble expansion data cannot be generalized to all low redshift data. Such situation is in contrast to type III and IV models, which are able to successfully fit the linear growth data at a similar quality level as the Λ CDM, as can also be appreciated in Fig. 1. In fact, the three curves corresponding to models III, IV and the Λ CDM (for the best fit values of the parameters in Table 1) lie almost on top of each other in that figure, whereas the curves for models I and II depart very openly from the group of Λ CDM-like models. For the former there is an evident defect of structure formation with respect to the Λ CDM, whilst for the latter there is a notable excess.

The large differences can be explained as follows. As we have seen before the ratio ρ_Λ/ρ_r for type-II models is far from 0, and negative, in the far past. Now, from the basic equations in Sect. 2 we find that during the matter-dominated epoch the acceleration of the expansion is given by $\ddot{a}/a = (4\pi G/3)(2\rho_\Lambda - \rho_m)$. Thus, a negative value of the vacuum energy density, $\rho_\Lambda < 0$, helps to slow down the expansion (it actually cooperates with gravitation and enhances the aggregation of matter into clusters). Actually, the vacuum energy of model II did not become positive until $H(\tilde{z}) = -\epsilon H_0/\nu \approx 4.13H_0$, what corresponds to a redshift $\tilde{z} = 3.204$. This is why we obtain larger values of the density contrast in comparison with the models that take $c_0 \neq 0$ (cf. Fig. 1). Later on the universe started to speed up, and the transition value from deceleration to acceleration is given by

$$z_{tr}^{(II)} = \left[\frac{2(\zeta - \Omega_m^0)}{(3\zeta - 2)\Omega_m^0} \right]^{2/3\zeta} - 1. \quad (56)$$

From the values of the fitted parameters in Table 1, we find $z_{tr} = 1.057$. Numerically, it is significantly larger than in the Λ CDM ($z_{tr} \simeq 0.69$, for the central fit value of Ω_m^0 quoted in Table 1). From this point onwards the type-II vacuum has been accelerating the universe and restraining the gravitational collapse, but it has left behind a busy history of structure formation triggered by the large growth rate $\delta_m(a) \sim a^{3\zeta-2} = a^{1.675}$ (cf. the fit value $\zeta = 1.225$ from Table 1). Such history is difficult to reconcile with the (much more moderate) one indicated by observations.

In the other extreme we have type-I model, showing a serious lack of structure formation as compared to the Λ CDM (cf. Fig. 1), despite for both models $\delta_m(a) \sim a$. We can also understand the reason as follows. Let us assume a common value of the density parameter Ω_m^0 (which is a good

approximation under the fitting strategy we have followed in Table 1). In that case Eq. (22) tells us that the ratio of their vacuum energy densities is: $\rho_{\Lambda}^I/\rho_{\Lambda}^{\Lambda CDM} = 1 + \Omega_m^0(a^{-3/2} - 1)$. Thus, during the past cosmic history the vacuum energy density for the type-I model is positive and always larger than in the concordance model, so we should expect a reduced growth rate as compared to the Λ CDM. This is confirmed in Fig. 1.

In the next section, we analyze the nonlinear perturbation effects at small scales and consider the different capability of the vacuum models under study to produce cluster-size halo structures in the universe. This study will give strength to the results obtained at the linear level.

5 Number counts analysis

In the previous section we have shown that the Λ CDM-like vacuum models III and IV deviate mildly from the concordance model when we consider the linear structure formation. While in the future it may be possible to resolve better these differences there is another useful strategy that can be adopted to magnify the differences to a larger degree. It is based on the clustering properties of the nonlinear regime at smaller scales and on counting the number of formed structures in each vacuum framework. Present X-ray and Sunyaev-Zeldovich surveys, such as eROSITA (Merloni et al, 2012) and SPT (Bleem et al, 2014), can be very helpful to test these models. The method ultimately relies on the Press and Schechter (PSc) formalism (Press & Schechter 1974) and generalizations thereof. We will apply it to the various models under study.

From that formalism one can predict the abundance of bound structures that have been formed by gravitational collapse. The comoving number density of collapsed objects at redshift z within the mass interval M and $M + dM$ takes on the form

$$n(M, z)dM = -\frac{\bar{\rho}_m(z)}{M} \frac{\ln \sigma(M, z)}{dM} f(\sigma; \delta_c), \quad (57)$$

where $\bar{\rho}_m$ is the comoving background density and $f(\sigma; \delta_c)$ is the PSc-function. An important parameter in it is the collapse density threshold δ_c , which we have computed numerically for our models in Fig. 2. In the original PSc-form, $f_{\text{PSc}}(\sigma; \delta_c) = \sqrt{2/\pi}(\delta_c/\sigma) \exp(-\delta_c^2/2\sigma^2)$. However, in the present work we adopt the improved one proposed by (Reed et al. 2007), which depends on several additional parameters. Finally, $\sigma^2(M, z)$ is the mass variance of the smoothed linear density field. In Fourier space it is given by:

$$\sigma^2(M, z) = \frac{D^2(z)}{2\pi^2} \int_0^\infty k^2 P(k) W^2(kR) dk. \quad (58)$$

In this expression, $D(z)$ is the linear growth factor of perturbations, i.e. $D(z) \equiv \delta_m(z)$, which we have computed before for our models, $P(k)$ is the CDM power-spectrum of the linear density field and finally we have the smoothing function $W(kR) = 3(\sin kR - kR \cos kR)/(kR)^3$, which is the Fourier transform of the following geometric top-hat function with spherical symmetry: $f_{\text{top hat}}(r) = 3/(4\pi R^3) \theta(1 - r/R)$, where θ is the Heaviside function. It contains on average a mass M within a comoving radius $R = (3M/4\pi\bar{\rho})^{1/3}$.

The CDM power spectrum $P(k) = P_0 k^{n_s} T^2(\Omega_m^0, k)$ is used, where P_0 is a normalization constant, and n_s is the spectral index given by $n_s = 0.9603 \pm 0.0073$ as measured by Planck+WP (Ade

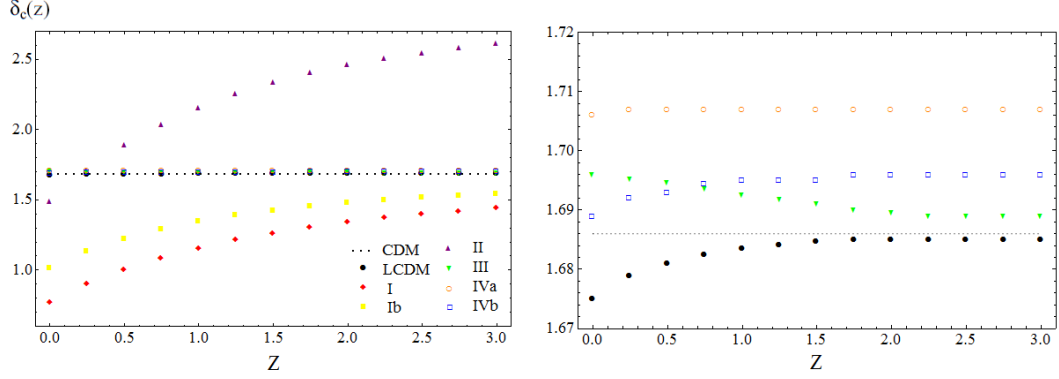


Figure 2: Computation of the collapse density threshold $\delta_c(z)$ using the best fit values shown in Table 1. With these values we solve numerically Eq. (41) following the procedure outlined in Appendix A of (Grande, Solà, Basilakos & Plionis 2011). In both plots we include the fiducial constant CDM value $\delta_c = \frac{3}{20}(12\pi)^{2/3} \approx 1.686$ (horizontal dotted line) and the Λ CDM curve (solid points, in black). The models with $c_0 \neq 0$ (i.e. III and IV) provide $\delta_c(z)$ very close to the Λ CDM model and the corresponding curves are cluttered in the plot on the left. In the right plot we zoom in the relevant region $\delta_c^{CDM} \pm_{-0.016}^{+0.024}$ in order to clearly appreciate the differences between them. In the plot on the left these differences cannot be seen owing to the large deviations shown by models I and II ($c_0 = 0$) which required to use a large span for the vertical axis. Finally, the curve indicated as Ib has been computed for model I under another set of inputs (cf. Appendix A of the current paper).

et al. 2013). Finally, $T(\Omega_m^0, k)$ is the BBKS transfer function (Bardeen, Bond, Kaiser & Szalay 1986; Liddle & Lyth 2000). Introducing the dimensionless variable $x = k/k_{eq}$, in which $k_{eq} = a_{eq}H(a_{eq})$ is the value of the wave number at the equality scale of matter and radiation, we can write the transfer function as follows:

$$T(x) = \frac{\ln(1 + 0.171x)}{0.171x} \left[1 + 0.284x + (1.18x)^2 + (0.399x)^3 + (0.490x)^4 \right]^{-1/4}.$$

It is important to emphasize that k_{eq} is a model dependent quantity. For type-III and type-IV models one can use the same formula that is obtained in the Λ CDM, due to the fact that the deviations are negligible in these cases, as we have checked. On the contrary, with type-I and type-II models we are not allowed to do that. We must derive the corresponding expression for k_{eq} by applying (38) and (39). The final results for each model read as follows:

$$(I) \quad k_{eq} = H_0 \sqrt{\frac{2}{\Omega_r^0}} (\Omega_m^0)^{4/3}, \quad (II) \quad k_{eq} = \frac{H_0 \sqrt{2}}{\zeta^{\frac{1}{3\zeta} + \frac{1}{2}}} (\Omega_m^0)^{2 - \frac{2}{3\zeta}} (\Omega_r^0)^{\frac{1}{\zeta} - \frac{3}{2}}, \quad (59)$$

and

$$(III, IV) \quad k_{eq} = H_0 \Omega_m^0 \sqrt{\frac{2}{\Omega_r^0}} e^{-\Omega_b^0 - \sqrt{2h} \frac{\Omega_b^0}{\Omega_m^0}}. \quad (60)$$

We normalize the power spectrum using σ_8 , the rms mass fluctuation amplitude on scales of $R_8 = 8 h^{-1}$ Mpc at redshift $z = 0$ [$\sigma_8 \equiv \sigma_8(0)$]. The σ_8 value for the different dynamical vacuum models can be estimated as in (Grande, Solà, Basilakos & Plionis 2011) by scaling the Λ CDM value $\sigma_{8,\Lambda} = 0.829 \pm 0.012$ extracted from (Ade et al. 2013). Upon using Eq. (58) with the CDM power spectrum the mass variance of the linear density field for each model can finally be computed as follows:

$$\frac{\sigma^2(M, z)}{\sigma_{8,\Lambda}^2} = \frac{D^2(z)}{D_{\Lambda}^2(0)} \frac{\int_0^\infty k^{n_s+2} T^2(\Omega_m^0, k) W^2(kR) dk}{\int_0^\infty k^{n_s+2} T^2(\Omega_{m,\Lambda}^0, k) W^2(kR_8) dk}. \quad (61)$$

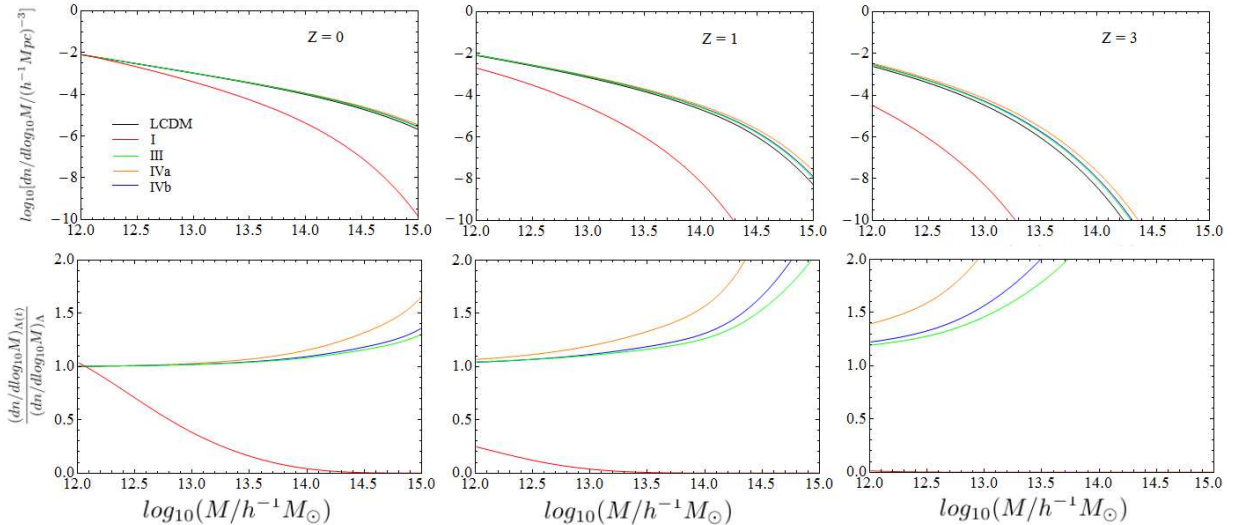


Figure 3: *Upper plots:* The differential comoving number density as a function of the halo mass for the various dynamical vacuum models and the concordance Λ CDM model at redshifts $z = 0$, $z = 1$ and $z = 3$, respectively. *Lower plots:* Corresponding differences in the comoving number density with respect to the Λ CDM model.

Using this procedure, along with the best-fit values of Table 1 and the numerically determined collapse density $\delta_c(z)$ (cf. Fig. 2) entering the generalized PSc-function $f(\sigma; \delta_c)$ of (Reed et al. 2007), we have computed the fractional difference $\delta\mathcal{N}/\mathcal{N}$ (where $\delta\mathcal{N} \equiv \mathcal{N} - \mathcal{N}_{\Lambda\text{CDM}}$) for the number counts of clusters between the dynamical vacuum models and the concordance Λ CDM one. The differential comoving number density of predicted cluster-size structures at particular values of the redshift ($z = 0, z = 1$ and $z = 3$), as well as the normalized results with respect to the corresponding Λ CDM prediction, are presented in Fig. 3, whereas in Fig. 4 we show the differences in the halo mass function through the comoving number density for the various models at two fixed redshifts ($z = 1$ and $z = 3$). Finally, in Fig. 5 we plot the redshift distribution of the total number of counts.

These figures encapsulate all the main information on the number counts analysis. They display the number of counts for each model per mass range at fixed redshift, and the total number of structures at each redshift within the selected mass range. The upshot from our analysis is that the models with $c_0 \neq 0$ predict either a very small (type-I) or a very large (type-II) number of clusters as compared to the Λ CDM. This is not surprising if we inspect the power for structure formation of these models in the linear perturbation regime (see Fig. 1 and the comments at the end of Sect. 4). As a result we deem unrealistic the situation for both the type I and type II models. When we translate this situation to the corresponding prediction for the number counts we find that, for model I, $\mathcal{N}^I/\mathcal{N}_{\Lambda\text{CDM}} \ll 1$, whereas for model II $\mathcal{N}^{II}/\mathcal{N}_{\Lambda\text{CDM}} \gg 1$ in the whole range. As a result, the former yields $\delta\mathcal{N}/\mathcal{N}_{\Lambda\text{CDM}} \rightarrow -1$ at increasing redshifts (as can be appreciated in Fig. 5), whereas the latter is out of the window under study.

In contrast, the situation with the Λ CDM-like models III and IV is quite encouraging. These models represent viable alternatives, at least from the phenomenological point of view, to the strictly rigid situation of the Λ CDM (in which $\rho_\Lambda = \text{const.}$ for the entire cosmic history). While

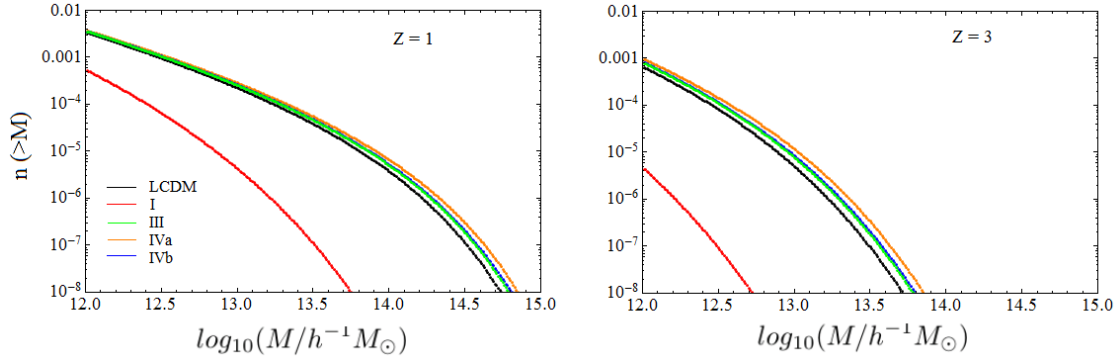


Figure 4: The comoving number density at two different redshifts for the different models.

these models depart only mildly from the Λ CDM predictions near our time, the differences become sizeable deep in the past, but still within bound. Concerning the number counts differences with respect to the concordance model we recognize from Fig. 5 significant ($\sim 20 - 30\%$) positive departures at moderate redshift ranges, where the total number of counts is still sizeable. Therefore the predicted deviations can be measured, in principle, and could be used as an efficient method to separate models III and IV.

6 Conclusions

In this work we have discussed a class of dynamical vacuum models whose energy density ρ_Λ contains a linear and a quadratic term in the Hubble rate, H , i.e. with the general structure: $\rho_\Lambda(H) = C_0 + C_1 H + C_2 H^2$. Models in this class having $C_0 \neq 0$ have a well-defined Λ CDM limit when the remaining parameters go to zero. These models are particularly interesting as they can have a Λ CDM-like behavior near our time but their dynamical nature can help to better explain the past cosmic history. A particular (but qualitatively different) subclass of dynamical models is those having $C_0 = 0$; despite they do not have a Λ CDM limit, models of this sort have been repeatedly invoked in the literature on several accounts. In particular, the pure linear model $\rho_\Lambda \propto H$ has been proposed by different authors trying to relate the value of the cosmological constant with QCD. It is therefore interesting to closely scrutinize the phenomenological situation of all these models in the light of the most recent cosmological data.

The net outcome of our investigation is the following. At leading order all these dynamical vacuum models can provide a consistent description of the cosmic evolution, but they exhibit some differences that can be checked observationally. On a deeper look, these differences can become quite significant. In particular, we have confronted the vacuum models against the structure formation data, and at the same time we have assessed their considerably different capability in populating the Universe with virialized (cluster-size) structures at different redshifts as compared to the Λ CDM model. While all these models can fit reasonably well the Hubble expansion data, those with $C_0 = 0$ (denoted as type I and II) are unable to account for the linear structure formation; and, at the same time, they lead to either an overproduction or to a drastic depletion

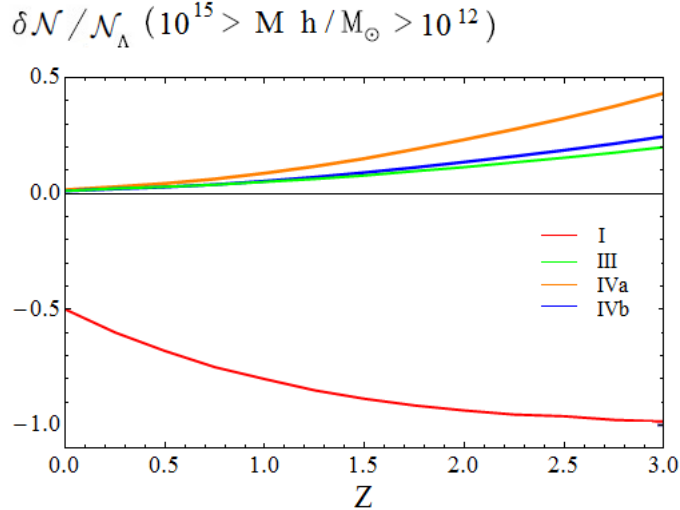


Figure 5: The fractional difference $\delta\mathcal{N}/\mathcal{N}_{\Lambda\text{CDM}}$ with respect to the ΛCDM model (where we have defined $\delta\mathcal{N} \equiv \mathcal{N} - \mathcal{N}_{\Lambda\text{CDM}}$). The curve for the type-II model is not plotted because it is out of range, i.e. $\delta\mathcal{N}/\mathcal{N} > 1$.

in the number of virialized structures as compared to the ΛCDM . In contrast, the $C_0 \neq 0$ models (types III and IV) perform at a comparable level to the ΛCDM and show measurable differences (cf. Fig. 5) that could possibly be pinned down in the near future in ongoing and planned surveys.

The current Universe appears in all these models as FLRW-like, except that the vacuum energy is not a rigid quantity but a mildly evolving one. For the $C_0 \neq 0$ models the typical values we have obtained for the coefficients ν and ϵ (responsible for the time evolution of ρ_Λ) lie in the ballpark of $\sim 10^{-3}$. This order of magnitude value is roughly consistent with the theoretical expectations, specially for the coefficient ν which can be linked in QFT with the one-loop β -function of the running cosmological constant. It is a rewarding feature since it points to a possible fundamental origin of the structure of these models in the context of QFT in curved spacetime. However, the presence of the linear term in H cannot be directly related to a similar QFT origin, although it could be associated to the presence of phenomenological bulk viscosity effects. We cannot exclude this possibility a priori and for this reason we have performed a thorough phenomenological analysis including this term in the general structure of the vacuum energy density. Our conclusion is that the linear term (parameterized by the coefficient ϵ) is currently tenable at the level $|\epsilon| \sim 10^{-3}$ provided $C_0 \neq 0$ (hence for type III and IV models only). For $C_0 = 0$, though, the large departure from the ΛCDM behavior is unacceptable both within the linear and nonlinear regimes.

To summarize, the wide class of dynamical vacuum models of the cosmic evolution with $C_0 \neq 0$ may offer an appealing and phenomenologically consistent perspective for describing dark energy. These models treat the vacuum energy density as a cosmic variable on equal footing to the matter energy density. In a context of an expanding universe this option may be seen as more reasonable than just postulating an everlasting and rigid cosmological term for the full cosmic history. Some of the models we have investigated mimic to a large degree the current behavior of the concordance ΛCDM model, but show measurable differences when we explore our past. Overall the dynamical vacuum models may eventually offer a clue for a better understanding of the origin of the Λ -term

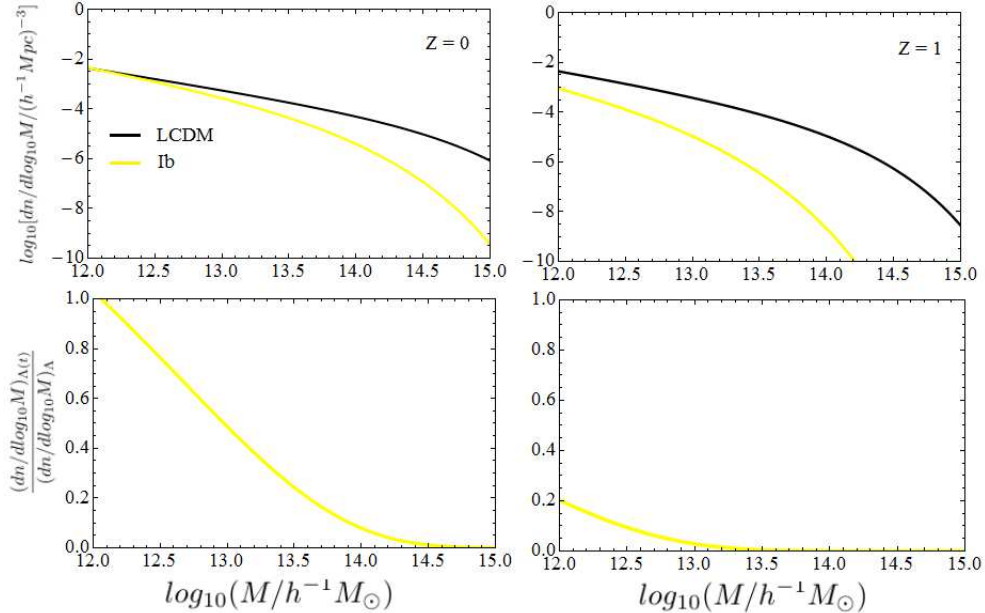


Figure 6: As in Fig.3, but for the parameters and the framework used in (Chandrachani et al. 2014) for $z = 0$ and $z = 1$. The curve indicated as Ib (showing a negative departure with respect to the Λ CDM) corresponds to the new evaluation of model I under the inputs indicated in the text of Appendix A. The corresponding collapse density threshold $\delta_c(z)$ for the new inputs is indicated in Fig. 2 also as Ib.

and the cosmological constant problem in the context of fundamental physics.

7 Acknowledgements

The work of AGV has been partially supported by an APIF predoctoral grant of the Universitat de Barcelona. JS has been supported in part by FPA2013-46570 (MICINN), Consolider grant CSD2007-00042 (CPAN) and by 2014-SGR-104 (Generalitat de Catalunya). We thank S. Basilakos for discussions.

A Number counts for $\rho_\Lambda \propto H$ under different inputs

In this appendix we briefly compare our results for the linear model, $\rho_\Lambda \propto H$ – model I in (5) – with those presented in (Chandrachani et al. 2014), where an excess in the number of counts was reported as compared with the Λ CDM. Here we try to use the parameters indicated by these authors (despite that not all of them are evident); in particular, we adopt at this point the halo mass function of (Sheth & Tormen, 1999). However, after all these changes we do not concur with their results and we find once more (as in the previous Fig. 3 for our original fitting parameters, with the halo mass function of Reed et al., 2007) a large deficit in the number of counts (cf. Fig. 6). Even neglecting the radiation corrections to the vacuum energy and adopting their ansatz $k_{eq} \propto (\Omega_m^0)^2$ and the quoted value for $\Omega_m^0 = 0.45$, we do not meet the claimed excess $\delta\mathcal{N} > 0$ for model I. We also find that by restricting our fit to CMB data only, the model yields a good quality

fit for $\Omega_m^0 \sim 0.6$, but only at the expense of a bad fit to SNIa/BAO. If, in addition, we attempt an overall fit to SNIa+BAO+CMB we find $\Omega_m^0 \sim 0.52$ with poor statistical quality ($\chi^2/\text{d.o.f.} \sim 1.3$). In short, we find very hard to obtain Ω_m^0 near 0.45 at an acceptable value of $\chi^2/\text{d.o.f.} < 1$. Even trying to mimic as much as possible the conditions used by the aforementioned authors we always find, in contrast to them, a large deficit in the number counts (see Fig. 6). Our results are consistent with the rather depleted linear growth behavior exhibited by model I in Fig. 1, which cannot be reconciled with $\delta\mathcal{N} > 0$ neither qualitatively nor quantitatively. Let us also note that our results for model II (which in this case do predict a large excess in the number of counts, for the fitted values in Table 1) are also consistent with the large enhancement of the growth rate displayed by model II in Fig. 1 as compared to the rest of the vacuum models, including the Λ CDM.

References

- [1] Ade P.A.R et al. [Planck Collaboration], *Planck 2013 results. XVI. Cosmological parameters*, Astron. Astrophys. (2014) [e-Print: arXiv:1303.5076].
- [2] Alcaniz J.S., Borges H.A., Carneiro S., Fabris J.C., Pigozzo C., & Zimdahl W, Phys.Lett. B716 (2012) 165 [e-Print: arXiv:1201.5919].
- [3] Bardeen J. M., Bond J. R., Kaiser N., & Szalay A. S., *Astrophys. J.*, **304** (1986) 15.
- [4] Barrow J. D., *Nucl. Phys.* **B310** (1988) 743.
- [5] Basilakos S., *Mon. Not. R. Astron. Soc.*, **395** (2009) 2347.
- [6] Basilakos S., Plionis M., & Solà J., 2009, *Phys. Rev. D.*, 80, 3511 [e-Print: arXiv:0907.4555]
- [7] Basilakos S., Polarski D., & Solà J., *Phys. Rev.* **D86** (2012) 043010 [e-Print: arXiv:1204.4806].
- [8] Basilakos S., & Solà J., *Phys. Rev.* **D90** (2014) 023008 [e-Print: arXiv:1402.6594].
- [9] Blake C. et al., *Mon. Not. Roy. Astron. Soc.*, **418** (2011) 1707 [e-Print: arXiv:1108.2635].
- [10] Bleem L.E. et al., e-Print: arXiv:1409.0850.
- [11] Borges H.A., Carneiro S., Fabris J. C., & Pigozzo C., *Phys. Rev. D.*, 77, 043513 (2008).
- [12] Chandrachani Devi N., Borges H.A., Carneiro S., & Alcaniz J.S. e-Print: arXiv:1407.1821.
- [13] Copeland E.J., Sami M., & Tsujikawa S., 2006, *Int. J. Mod. Phys.* **D 15**, 1753.
- [14] Eisenstein D. J. et al., (SDSS Collab.), *Astrophys. J.*, **633** (2005) 560.
- [15] España-Bonet C. et al., *JCAP* **0402** (2004) 006; *Phys.Lett.* **B574** (2003) 149.
- [16] Gómez-Valent A., Solà J., & Basilakos S., *JCAP* **01** (2015) 004 [e-Print: arXiv:1409.7048].
- [17] Grande J., Solà J., Basilakos S., & Plionis M., *JCAP* 08 2011 007 [e-Print: arXiv:1103.4632].

- [18] Hu W., & Sugiyama N., *Astrophys. J.* **444** (1995) 489 [e-Print: astro-ph/9510117].
- [19] Jesus J.F., Oliveira F.A., Basilakos S., & Lima J.S., *Phys. Rev. D* **84** (2011) 063511 [arXiv:1105.1027 [astro-ph.CO]].
- [20] Klinkhamer F.R., & Volovik G.E., *Phys.Rev.* **D79** (2009) 063527
- [21] Komatsu N., & Kimura S., *Phys.Rev.* **D88** (2013) 083534 [e-Print: arXiv:1307.5949].
- [22] Liddle A.R., & Lyth D.H., *Cosmological Inflation and Large-Scale Structure* (Cambridge Univ. Press, 2000).
- [23] Lima J. A. S., Basilakos S., & Solà J., 2013, *MNRAS*, 431 [e-Print: arXiv:1209.2802]; *Non-singular Decaying Vacuum Cosmology and Entropy Production* [e-Print: arXiv:1412.5196]
- [24] Merloni et al., e-Print: arXiv:1209.3114;
- [25] Ohta N., *Phys. Lett. B* **695** (2011) 41.
- [26] Pace F., Waizmann J.-C, & Bartelmann M., *Mon. Not. Roy. Astron. Soc.* **406**20101865 [e-Print: arXiv:1005.0233].
- [27] Padmanabhan T., *Phys. Rep.* **380** (2003) 235.
- [28] Peebles P. J. E., *Principles of Physical Cosmology* (Princeton Univ. Press, Princeton New Jersey, 1993).
- [29] Peebles P.J.E., & Ratra B., *Rev. Mod. Phys.* **75** (2003) 559.
- [30] Perlmutter S. et al. [Supernova Cosmology Project Collaboration], *Astrophys. J.* **517** (1999) 565 [astro-ph/9812133].
- [31] Press W.H., & Schechter P., *Astrophys. J.* **187** (1974) 425.
- [32] Reed D., Bower R., Frenk C., Jenkins A., & Theuns T., *MNRAS* **374** (2007) 2 [e-Print: astro-ph/0607150].
- [33] Ren J., & Meng X-H., *Phys. Lett. B***633** (2006) 1 [e-Print: astro-ph/0511163]; *Int. J. Mod. Phys. D***16** (2007) 1341 [e-Print: astro-ph/0605010].
- [34] Riess A. G. et al. [Supernova Search Team Collaboration], *Astron. J.* **116** (1998) 1009 [astro-ph/9805201].
- [35] Schutzhold R., *Phys. Rev. Lett.* **89** (2002) 081302 [e-Print: gr-qc/0204018].
- [36] Shaefer D.L., & Huterer D., *Phys.Rev.* **D89** (2014) 063510 [e-Print:arXiv:1312.1688].
- [37] Shapiro I.L., & Solà J., *JHEP* **0202** (2002) 006 [e-Print: arXiv:hep-th/0012227].
- [38] Shapiro I.L., & Solà J., *PoS AHEP2003* (2003) 013 [e-Print: astro-ph/0401015].

- [39] Shapiro I.L., & Solà J., Nucl. Phys. Proc. Suppl. **127** (2004) 71 [e-Print: hep-ph/0305279].
- [40] Shapiro I.L., & Solà J., Phys. Lett. B **682** (2009) 105 [e-Print: arXiv:0910.4925].
- [41] Sheth R.K., & Tormen G., Mon. Not. Roy. Astron. Soc. **308** (1999) 119 [e-Print: astro-ph/9901122].
- [42] Solà J., J. of Phys. **A41** (2008) 164066 [e-Print: arXiv:0710.4151].
- [43] Solà J., *Cosmological constant and vacuum energy: old and new ideas*, J. Phys. Conf. Ser. (2013) **453** 012015 [e-Print: arXiv:1306.1527].
- [44] Solà J., *Cosmologies with a time dependent vacuum*, J. Phys. Conf. Ser. (2011) **283** 012033 [e-Print: arXiv:1102.1815].
- [45] Solà J., Gómez-Valent A., *The $\bar{\Lambda}$ CDM cosmology: from inflation to dark energy through running Λ* , Int. J. of Mod. Phys. **D24** (2015) 1541003 [e-Print: arXiv:1501.03832].
- [46] Solà J., & Štefančić H., Phys. Lett. **B624** (2005) 147 [e-Print: astro-ph/0505133].
- [47] Solà J., & Štefančić H., Mod. Phys. Lett. **A21** (2006) 479 [e-Print: astro-ph/0507110].
- [48] Suzuki N., Rubin D., Lidman C., Aldering G., Amanullah R., Barbary K., Barrientos L.F., & Botyanszki J. et al., Astrophys. J **746** (2012) 85.
- [49] Thomas E.C., Urban F.R., & Zhitnitsky A.R., JHEP **0908** (2009) 043.
- [50] Weinberg S., Rev. Mod. Phys. **61** (1989) 1.
- [51] Zimdahl W., Phys. Rev. **D53** (1996) 5483.